Journal of Molecular Spectroscopy 273 (2012) 30–33

Contents lists available at SciVerse ScienceDirect

Journal of Molecular Spectroscopy

journal homepage: www.elsevier.com/locate/jms

High resolution Fourier transform emission spectroscopy of the $A^2\Pi$–$X^2\Sigma^+$ and $B^2\Sigma^+$–$X^2\Sigma^+$ systems of the $^{12}C^{15}N$ free radical

Reginald Colin [a], Peter F. Bernath [b,c,*]

[a] Service de Chimie Quantique et Photophysique, Université Libre de Bruxelles (ULB), 50, av. F.D. Roosevelt, 1050 Brussels, Belgium
[b] Department of Chemistry and Biochemistry, Old Dominion University, Norfolk, VA 23529, USA
[c] Department of Chemistry, University of York, Heslington, York YO10 5DD, UK

ARTICLE INFO

Article history:
Received 30 December 2011
In revised form 28 January 2012
Available online 5 March 2012

Keywords:
Spectroscopy
Free radical
Spectroscopic constants

ABSTRACT

Emission spectra of the $A^2\Pi$–$X^2\Sigma^+$ (red) and $B^2\Sigma^+$–$X^2\Sigma^+$ (violet) systems of the $^{12}C^{15}N$ molecule have been investigated in the 4500–26 000 cm^{-1} spectral region at high resolution using a Fourier transform spectrometer. In all, 22 bands of the A–X system and six bands of the B–X system have been rotationally analyzed providing a set of molecular constants for the v'' = 0–5, v' = 0–4 and v' = 0–3 levels of the X, A and B states, respectively.

1. Introduction

In 1940, CN was one of the first molecules to be discovered in interstellar space [1]. Since then, it has been shown to be present in many extraterrestrial objects (stars and comets) and in flames, and has been extensively studied in the laboratory. The most recent high resolution spectroscopic investigations of the $A^2\Pi$–$X^2\Sigma^+$ and $B^2\Sigma^+$–$X^2\Sigma^+$ systems of the main $^{12}C^{14}N$ isotopologue are those of Ram et al. [2,3] which include a review of previous studies of this radical. The $A^2\Pi$–$X^2\Sigma^+$ [4] and $B^2\Sigma^+$–$X^2\Sigma^+$ [5] systems of the $^{13}C^{14}N$ isotopologue have also been analyzed recently. Very few studies [6,7] concern the properties of the less abundant $^{12}C^{15}N$ isotopic form. In particular, the N = 2–1 rotational transition has been detected in Orion A by radio astronomers [6], and the fundamental vibration–rotation band has been measured in the laboratory by diode laser spectroscopy [7]. Precise high resolution spectroscopic parameters are however required in astrophysics in order to study the relative abundance of the ^{15}N atom in various celestial bodies [8,9].

The most important application of the spectroscopy of $C^{15}N$ is to measure the isotopic $^{14}N/^{15}N$ abundance ratio in comets [8–10]. The relative line intensities of the CN isotopologues in the $B^2\Sigma^+$–$X^2\Sigma^+$ transition have demonstrated that all comets have a $^{12}C/^{13}C$ abundance ratio of about 90 similar to that on Earth. The $^{14}N/^{15}N$ abundance ratio, however, is about 140, with ^{15}N enriched by nearly a factor of two compared to the terrestrial value [9,10]. Isotopic ratios can be used to test the hypothesis that comets have delivered a substantial amount of water to the Earth. The observed isotopic abundances of nitrogen are consistent with only a small cometary contribution of water to the Earth [10].

This work analyzes the A–X and B–X band systems of $^{12}C^{15}N$ in order to yield precise molecular constants for the three states involved.

2. Experimental details

The CN spectra were recorded by J. Brault (deceased) and R. Engleman on 1 September, 1977 (#3, 4 and 6) using the Fourier transform spectrometer associated with the McMath–Pierce Solar Telescope of the National Solar Observatory. The $C^{15}N$ radicals were made in a microwave discharge of argon, $^{15}NH_3$(?) and methane. The spectra were recorded in three parts using the visible beamsplitter; each part consisted of the co-addition of 8 scans in 1 h. The first part covered the 2900–12 000 cm^{-1} region with an InSb detector and a GaAs filter at 0.015 cm^{-1} resolution. The middle region (8500–22 000 cm^{-1}) used a Si photodiode detector and a GG475 filter at 0.031 cm^{-1} resolution. The high wavenumber region (20 000–28 000 cm^{-1}) used a Si photodiode detector with 450 nm violet pass and Corning 4–96 filters at 0.055 cm^{-1} resolution.

3. Observations

Based on a comparison with the bands of the A–X (red) and B–X (violet) systems of $^{12}C^{14}N$ [2,3] present in the spectrum, the

* Corresponding author at: Department of Chemistry and Biochemistry, Old Dominion University, Norfolk, VA 23529-0126, USA. Fax: +1 757 683 4628.
E-mail address: pbernath@odu.edu (P.F. Bernath).

0022-2852/$ - see front matter © 2012 Elsevier Inc. All rights reserved.
doi:10.1016/j.jms.2012.01.007

following bands of $^{12}C^{15}N$ were readily identified in the regions of 4500–16 000 cm^{-1} and 23 700–26 000 cm^{-1} respectively:

$A^2\Pi–X^2\Sigma^+$: 0–0, 0–1, 0–2, 1–0, 1–1, 1–2, 1–3, 2–0, 2–1, 2–2, 2–3, 2–4, 3–0, 3–1, 3–2, 3–3, 3–4, 3–5, 4–0, 4–1, 4–2 and 4–4

$B^2\Sigma^+–X^2\Sigma^+$: 0–0, 0–1, 1–1, 1–2, 2–3 and 3–4

The isotopic intensity ratio $^{12}C^{15}N/^{12}C^{14}N$ was ~1.7.

Approximate vibrational and rotational constants for the X, A and B states of $^{12}C^{15}N$ were calculated using the usual isotopic relations and the literature data for $^{12}C^{14}N$ [2,3]. Inserting these into the PGOPHER program [11], the rotational lines of the observed bands of both transitions for both isotopic species were computed and compared to the new spectrum. The rotational lines of the 22 bands of the $A^2\Pi–X^2\Sigma^+$ and the 6 bands of the $B^2\Sigma^+–X^2\Sigma^+$ of $^{12}C^{15}N$ were easily identified. For the A–X bands the 12 expected branches were found except that for the higher vibrational bands, the weaker satellite branches $^{O}P_{12}$ and $^{S}R_{21}$were sometimes absent. For the B–X bands, the four expected branches were identified except for the weaker 2–3 and 3–4 bands for which only the $^{R}R_{11}$ and $^{R}R_{22}$ branches were found. Fig. 1 shows a portion of the 0–0 band of the $A^2\Pi–X^2\Sigma^+$ system and Fig. 2 shows that of the 0–1 band of the $B^2\Sigma^+–X^2\Sigma^+$ system. A careful calibration of the spectrum was carried out by an adjustment to the $^{12}C^{14}N$ line positions of Ram et al. [2,3]. In the region of the A–X system there remains many weak unassigned lines showing no obvious structure. They are most likely due to bands of this system with higher v' which are known to be perturbed [3].

4. Results and discussion

The bands of the $A^2\Pi–X^2\Sigma^+$ system were rotationally analyzed using the PGOPHER program [11] which uses the effective N^2 Hamiltonian of Brown et al. [12]. In a first step, each band was fitted separately and adjustments to the line identifications were made. Finally all 22 bands (8074 lines) were fitted simultaneously yielding the 31 constants for the $X^2\Sigma^+$ state given in Table 1 and the 46 constants for the $A^2\Pi$ state given in Table 2. One standard deviation error estimates in parentheses refer to the last digits. The vacuum wave numbers of the measured lines along with the observed-calculated values can be found in the Appendix of this report. The average error of the fitted lines is 0.007 cm^{-1}.

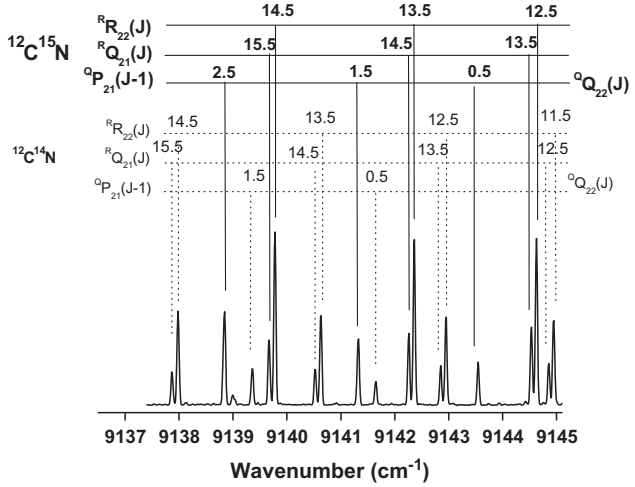

Fig. 1. Portion of the 0–0 band of the $A^2\Pi–X^2\Sigma^+$ transition.

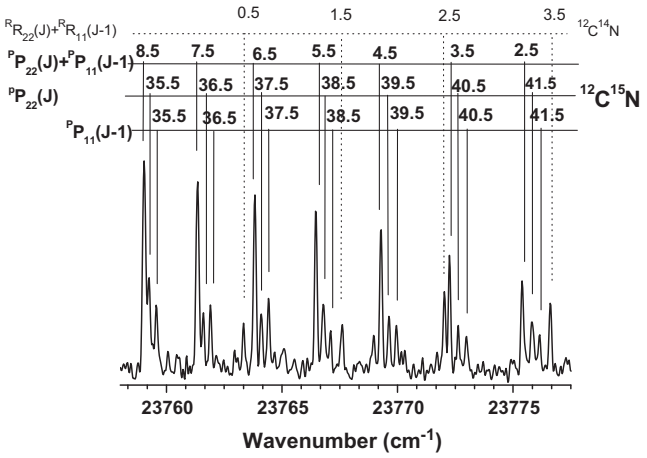

Fig. 2. Portion of the 0–1 band of the $B^2\Sigma^+–X^2\Sigma^+$ transition.

A similar procedure was adopted to analyze the six $B^2\Sigma^+–X^2\Sigma^+$ bands involving 491 lines, but due to the fact that no satellite $^{R}Q_{21}$ or $^{P}Q_{12}$ branches linking the F_1 and F_2 components were observed and only one band involving $v' = 2$ and one involving $v' = 3$ were recorded, it was decided to keep the lower ground state constants equal to those derived from the A–X analysis. This allowed us to derive spin-spitting constants for each vibrational level of the B state and to link together the four vibrational levels observed. The resulting constants for the $B^2\Sigma^+$ state are presented in Table 3. The vacuum wavenumber and the observed-calculated value of each fitted line are given in the Appendix. The average error of the fitted lines is 0.02 cm^{-1}.

In the previous studies, the A–X and B–X transitions of the $^{12}C^{14}N$ isotopologue [2,3] perturbations have been shown to be present in all three states. For the X ground state perturbations are present on the $v'' = 11$ level whereas strong interactions between the A and B states start to appear at lower v values ($v > 8$ for A and $v > 5$ for B). Similar interactions most certainly exist in the states of $^{12}C^{15}N$ and explain the difficulty in identifying other bands of both systems in the present spectrum, which has both isotopologues overlapping with similar intensities.

The spectroscopic constants of Tables 1–3 were used to calculate the principal equilibrium constants and the equilibrium internuclear distance (Table 4) of the three states involved using the following expressions:

$$G(v) = \omega_e(v+1/2) - \omega_e x_e(v+1/2)^2 + \omega_e y_e(v+1/2)^3 + \omega_e z_e(v+1/2)^4 \quad (1)$$

$$A_v = A_e + \alpha_{A1}(v+1/2) + \alpha_{A2}(v+1/2)^2 + \alpha_{A3}(v+1/2)^3 \quad (2)$$

$$B_v = B_e + \alpha_1(v+1/2) + \alpha_2(v+1/2)^2 + \alpha_3(v+1/2)^3 \quad (3)$$

The following theoretical isotope relation values in which $i = {}^{12}C^{14}N$ and $j = {}^{12}C^{15}N$ and μ is the reduced mass of the molecule,

$$\omega_e^i/\omega_e^j = (\mu^j/\mu^i)^{1/2} = 1.0156977 \quad (4)$$

$$B_e^i/B_e^j = (\mu^j/\mu^i) = 1.0316418 \quad (5)$$

were compared with the values obtained using the present results and those of $^{12}C^{14}N$ [2,3]. Due to irregularities in the variation of the molecular constants for the B state with v [2], only the X and A states were examined. Eq. (4) yields for the $X^2\Sigma^+$ and $A^2\Pi$ states 1.0157036 and 1.0156901 respectively and Eq. (5) yields 1.0316337 and 1.0316247, respectively.

Table 1
Molecular constants for the $X^2\Sigma^+$ state of $^{12}C^{15}N$ (cm^{-1}).

v	0	1	2	3	4	5
T_v	0	2011.25212(55)	3997.02219(56)	5957.26933(62)	7891.95201(70)	9801.0250(16)
B	1.8332418(49)	1.8166148(49)	1.79991641(50)	1.7832011(51)	1.7664170(54)	1.749655(19)
$D \times 10^6$	6.0497(30)	6.0600(29)	6.0605(32)	6.0753(34)	6.0879(44)	6.242(44)
$H \times 10^{11}$	1.302(74)	1.327(74)	1.309(83)	1.153(93)	1.07(14)	0.8[a]
$\gamma \times 10^3$	6.975(30)	6.952(30)	6.916(31)	6.810(39)	6.757(26)	6.7[a]
$\gamma_D \times 10^8$	−6.3(21)	−8.6(21)	−11.3(22)	−12.7(29)	−20.0[a]	−30.0[a]

[a] Fixed.

Table 2
Molecular constants for the $A^2\Pi$ state of $^{12}C^{15}N$ (cm^{-1}).

v	0	1	2	3	4
T_v	9117.57002(58)	10878.05384(55)	12613.74846(52)	14324.64649(50)	16010.73393(56)
A	−52.65756(79)	−52.58594(71)	−52.51210(69)	−52.43634(64)	−52.35861(82)
$A_D \times 10^4$	−1.982(14)	−1.931(13)	−1.870(15)	−1.786(12)	−1.631(25)
B	1.65494116(52)	1.63845740(51)	1.6219255(45)	1.6053494(45)	1.5887337(46)
$D \times 10^6$	5.8045(35)	5.8188(33)	5.8252(17)	5.8384(17)	5.8525(17)
$H \times 10^{11}$	1.122(90)	1.241(86)	1.0[a]	1.0[a]	1.0[a]
$p \times 10^3$	8.107(64)	8.074(59)	8.123(64)	8.123(54)	8.037(59)
$p_D \times 10^7$	−2.68(45)	−2.71(41)	−4.03(52)	−4.07(39)	−4.0[a]
$q \times 10^4$	−3.678(16)	−3.721(15)	−3.821(18)	−3.914(17)	−4.046(21)
$q_D \times 10^8$	1.026(91)	0.913(84)	1.17(12)	1.057(81)	1.0[a]

T_v measured from the $X^2\Sigma^+$ F_{1e} $J = 0.5$ level.
[a] Fixed.

Table 3
Molecular constants for the $B^2\Sigma^+$ state of $^{12}C^{15}N$ (cm^{-1}).

v	0	1	2	3
T_v	25797.1828(24)	27888.5536(28)	29943.5774(59)	31955.4419(74)
B	1.898798(12)	1.879021(19)	1.853001(55)	1.831127(87)
$D \times 10^6$	6.226(15)	6.275(25)	6.414(81)	5.22(13)
$\gamma \times 10^2$	1.5567(87)	1.677(18)	0.243(43)	1.03(11)

$H(v = 0) = 8.6(49)\ 10^{-12}\ cm^{-1}$.

Table 4
Equilibrium constants for the $X^2\Sigma^+$, $A^2\Pi$ and $B^2\Sigma^+$ states of $^{12}C^{15}N$ (cm^{-1}).

	$X^2\Sigma^+$	$A^2\Pi$	$B^2\Sigma^+$
T_e	0	9243.177(7)	26653.1(5)
ω_e	2036.698(1)	1785.277(3)	2127.7[a]
$\omega_e x_e$	12.7129(9)	12.386(2)	18.2[a]
$\omega_e y_e$	−0.00599(9)	−0.0178(2)	–
$\omega_e z_e$	−0.00009(3)	–	–
A_e	–	−52.69254(10)	–
α_{A1}	–	0.06937(17)	–
α_{A2}	–	0.001170(80)	–
$\alpha_{A3} \times 10^5$	–	−2.1(11)	–
B_e	1.841530(2)	1.663170(3)	1.911(2)
α_1	−0.01655(4)	−0.016440(3)	−0.0229(8)
$\alpha_2 \times 10^5$	−4.4(14)	−2.20(5)	–
$\alpha_3 \times 10^6$	2.9(15)	–	–
r_e (Å)	1.171822(2)	1.233056(2)	1.150(2)

[a] Using $v = 0$ to 2 only.

Finally, the rotational term values for all the observed vibrational levels of the $X^2\Sigma^+$, $A^2\Pi$ and $B^2\Sigma^+$ states were calculated using the spectroscopic constants found in the final fits and are available in the Supplementary information. The term values of the $v = 0$ level of the $X^2\Sigma^+$ state allow us to calculate the fundamental infrared band and to compare our results with the direct measurements of the 21 lines by Hubner et al. [7]. The average agreement is 0.003 cm^{-1}.

Acknowledgments

The research in Belgium was funded by the FRS-FNRS. Financial support by the «Actions de Recherche Concertées» (Communauté Française de Belgique) is also acknowledged. Some support was provided by the Leverhulme Trust through a Research Project Grant and the NASA laboratory astrophysics program. We also wish to thank Dr. C. Western (University of Bristol, UK) for providing the latest version of the PGOPHER program. We thank R.S. Ram for help in locating the $^{12}C^{15}N$ spectra in the data archive of the National Solar Observatory.

Appendix A. Supplementary material

Supplementary data for this article are available on ScienceDirect (www.sciencedirect.com) and as part of the Ohio State University Molecular Spectroscopy Archives (http://library.osu.edu/sites/msa/jmsa_hp.htm). Supplementary data associated with this article can be found, in the online version, at doi:10.1016/j.jms.2012.01.007.

References

[1] A. McKellar, Publ. Astron. Soc. Pac. 52 (1940) 187–192.
[2] R.S. Ram, L. Wallace, P.F. Bernath, J. Mol. Spectrosc. 263 (2010) 82–88.
[3] R.S. Ram, S.P. Davis, L. Wallace, R. Engleman, D.R. Appadoo, P.F. Bernath, J. Mol. Spectrosc. 263 (2006) 247–253.

[4] R.S. Ram, L. Wallace, K. Hinkle, P.F. Bernath, Astrophys. J. Suppl. 188 (2010) 500–505.
[5] R.S. Ram, P.F. Bernath, Astrophys. J. Suppl. 194 (2011) 34. 6pp.
[6] A.H. Saleck, R. Simon, N. Schneider, G. Winnerwisser, Astrophys. J. 414 (1993) L133–L136.
[7] H. Hubner, M. Castillo, P.B. Davies, J. Ropcke, Spectrochem. Acta A61 (2005) 57–60.
[8] S. Wyckoff, M. Kleine, B.A. Peterson, P.A. Wehinger, L.M. Ziurys, Astrophys. J. 535 (2000) 991–999.
[9] D. Hutsemékers, J. Manfroid, E. Jehin, C. Arpigny, A. Cochran, R. Schultz, J.A. Shüwe, J.M. Zucconi, Astron. Astrophys. 440 (2005) L21–L24.
[10] D. Hutsemékers, J. Manfroid, E. Jehin, C. Arpigny, Icarus 204 (2009) 346–348.
[11] PGOPHER, A Program for Simulating Rotational Structure, C.M. Western, University of Bristol. <http://pgopher.chem.bris.ac.uk/>.
[12] J. Brown, E.A. Colbourne, J.K.G. Watson, F.D. Wayne, J. Mol. Spectrosc. 74 (1979) 294–318.